Towards an understanding of light activation processes in titanium oxide based inverted organic solar cells

Sylvain Chambon, Elodie Destouesse, Bertrand Pavageau, Lionel Hirsch, Guillaume Wantz

AIP | Journal of Applied Physics

Towards an understanding of light activation processes in titanium oxide based inverted organic solar cells

S. Chambon, E. Destouesse, B. Pavageau, L. Hirsch, and G. Wantz

Citation: J. Appl. Phys. **112**, 094503 (2012); doi: 10.1063/1.4764026
View online: http://dx.doi.org/10.1063/1.4764026
View Table of Contents: http://jap.aip.org/resource/1/JAPIAU/v112/i9
Published by the American Institute of Physics.

Towards an understanding of light activation processes in titanium oxide based inverted organic solar cells

S. Chambon,[1] E. Destouesse,[1] B. Pavageau,[2] L. Hirsch,[1] and G. Wantz[1,a)]
[1]*Univ. Bordeaux, IMS, UMR 5218, F-33400 Talence, France and CNRS, IMS, UMR 5218, F-33400 Talence, France*
[2]*Univ. Bordeaux, LOF, UMR 5258, F-33600 Pessac, France; CNRS, LOF, UMR 5258, F-33600 Pessac, France; and RHODIA, LOF, UMR 5258, F-33600 Pessac, France*

(Received 14 June 2012; accepted 9 October 2012; published online 5 November 2012)

The light activation phenomenon in inverted P3HT:PCBM bulk heterojunction organic solar cells based on titanium oxide sublayer (TiO_x) is characterized by fast acquisition of current-voltage (J-V) curves under light bias as function of time. TiO_x layers were thermally treated under inert atmosphere at different temperatures prior active layer deposition and for every device an activation time was extracted. It is shown that the higher the TiO_x annealing temperature, the faster the activation. The improvement of the overall device performances is also observed for devices with TiO_x layers baked above 100 °C. The evolution of the characteristic of the organic semiconductors (OSC) device, from dielectric to diode, is attributed to the increase of TiO_x conductivity by three orders of magnitude upon white light illumination. Additionally, devices based on baked TiO_x present higher conductivity than those based on unbaked TiO_x which would explain the gain in performances and the short activation time of the OSC. In order to understand the origin of the phenomenon, deactivation experiments were also performed under different conditions on OSC. The deactivation process was shown to be thermally dependent and fully reversible under inert atmosphere, which suggest that deep traps are responsible for the activation phenomenon. An optimal annealing temperature was found at 120 °C and gives a reasonable short activation time of approximately 1 min and photo conversion efficiency up to 4%. © *2012 American Institute of Physics*. [http://dx.doi.org/10.1063/1.4764026]

I. INTRODUCTION

Polymer photovoltaic solar cells (PSC) have been the subject of increasing attention around the world for the last 20 years as a potential source of renewable energy. PSC offer multiple advantages such as low production costs, reduced weight, potential flexibility, and power conversion efficiencies (PCE) approaching values of amorphous silicon industry.[1] Since 2005, so-called inverted PSC have been developed which exhibit improved air stability compared to conventional direct structures.[2–5] In an inverted PSC, electrons are collected by the indium tin oxide (ITO) bottom electrode through transparent electron selective layers, whereas holes are collected from the evaporated top electrode, generally across a thin film of hole selective layer such as molybdenum oxide (MoO_3) or poly(3,4-ethylenedioxythiophene) doped with poly(4-styrenesulfonate) (PEDOT-PSS). The top electrode is generally made of silver, since air exposure leads to the formation of silver oxide; the latter exhibits a higher work function thus enhancing hole collection.[6] Several materials such as calcium,[7,8] titanium oxide (TiO_x),[9,10] zinc oxide (ZnO),[11–13] cesium carbonate (Cs_2CO_3),[14,15] or aluminum-doped zinc oxide[9] have been introduced as transparent electron-selective layers. S-shape current-voltage (IV) curves or inflection points in direct solar cells have been observed and reported in various articles.[16,17] These authors attributed this phenomenon to the presence of strong interface dipoles or spaces charges due to a reduced majority surface recombination velocity. Similar inflection points can be observed in inverted solar cells build on ZnO and TiOx layers. In many cases, inverted solar cells built using TiO_x or ZnO present similar S-shaped IV characteristics which can be suppressed under continuous white light illumination. Such activation of inverted solar cells has been reported in a few articles for TiO_x based[18–21] as well as in ZnO based devices.[22–26] The commonly accepted explanation for ZnO activation is that adsorbed molecular oxygen acts as an electron trap and causes bending of the titania band diagram, therefore forming a barrier against the extraction of electrons. Upon UV illumination (part of the white light illumination of a sunlight or solar simulator), this adsorbed species desorbs and the charge extraction is enhanced, explaining the improvement of the fill factor.[22–26] However, in the case of TiO_x, the origin of the phenomenon is still under debate. While some groups claim that activation comes from adsorbed molecular oxygen (as for ZnO),[21,27] Kim *et al.* support the hypothesis that shallow charge carrier traps are present in between the valence band and the conduction band of TiO_x, which are filled upon UV irradiation of the TiO_x layer, therefore improving its series resistance and photo-conductivity.[20] Whatever the physical origin, improvement of the fill factor results in the disappearance of the insulating zone at one interface.

In this article, we attempt to give some insights on the light activation phenomenon. The light activation duration is studied via fast current-voltage measurements as a function

a)Author to whom correspondence should be addressed; Electronic mail: guillaume.wantz@ims-bordeaux.fr.

of thermal treatment of the oxide under inert atmosphere prior to the deposition of the bulk heterojunction. For every sample, the evolution of various photovoltaic parameters (J_{sc}, V_{oc}, FF, PCE) as a function of the irradiation time is plotted in order to extract a corresponding rising time. Fully activated devices are submitted to different storage conditions in order to study the deactivation of the device and understand the origin of the traps. Pure TiO_x-based devices were also fabricated in order to study the influence of the thermal treatment on the conductivity of the TiO_x layer.

II. MATERIALS AND METHODS

The bulk heterojunction used in this study is based on a well-known couple of materials: poly(3-hexylthiophene) (P3HT) and 1-(3-methoxycarbonyl)propyl-1-phenyl[6,6]C_{61} (PCBM), which has been extensively studied in the last decade.[28] Inverted solar cells have been fabricated with the structure Glass/ITO/TiO_x/P3HT:PCBM/MoO_3/Ag using standard procedures. 15×15 mm^2 ITO-coated glass sheets (10 Ω^2, *Kintec*) are successively cleaned in acetone, ethanol, and isopropanol in an ultrasonic bath and exposed to UV-ozone for 20 min. Titanium oxide is prepared as followed: Titanium (IV) isopropoxide (TIPT, Aldrich, 99.999%) is diluted in absolute ethanol at a concentration of 0.05 M, to which HCl is added in order to have a water to TIPT molar ratio (rw) of 0.82 and a *p*H of 1.9.[29] The precursor solution is stirred for 72 h at room temperature. 40 μl of TiO_x solution is spincoated on the substrate in air (ambient atmosphere) at 1000 rpm for 60 s and kept in air at room temperature for 2 h. Subsequently, the substrates were transferred to a nitrogen-filled glovebox (O_2 and H_20 < 0.1 ppm). Starting from this point, the rest of the fabrication process and all the I(V) characterizations are carried out under inert atmosphere. TiO_x coated ITO sheets were then thermally treated at various temperatures from 80 °C to 180 °C for 10 min on temperature-controlled hot plate. The TiO_x thickness was measured to be 15 ± 5 nm using a *Tencor IQ* profilometer. P3HT (*Plexcore OS2100*) and PCBM (99.5%) were supplied from *Plextronics* and *Solaris-Chem Inc*., respectively, and used as received. Solutions were prepared in o-dichlorobenzene, at a 1:1 weight ratio and a concentration of 20 mg/ml. Solutions were first stirred at 90 °C for 10 min and subsequently at 50 °C for 24 h. P3HT:PCBM was spincoated at 1000 rpm during 25 s. Instantly after spin-coating, the substrates were individually placed in small closed petri dishes overnight at room temperature for solvent annealing. Solvent annealing is a well-known technique to promote the phase segregation of bulk-heterojunction materials by keeping the layers under a saturated solvent atmosphere.[30] It is important to mention that no thermal annealing of BHJ was performed in this study, in order to increase the effect of temperature on TiO_x only. The resulting P3HT:PCBM thickness was 240 ± 10 nm. Both the solvent annealing procedure and the spincoating time coupled to solution concentration, i.e., active layer thickness, were optimized. 8 nm-thick MoO_3 (*Serac*) followed by 100 nm-thick silver electrodes were successively thermally evaporated under a secondary vacuum (10^{-6} mbar) onto the P3HT:PCBM layer through a shadow mask to define a 8.6 mm^2 active area. Experiments were repeated on 8 individual cells to evaluate the standard deviation. The devices were characterized using a *K.H.S. Solar-Celltest- 575* solar simulator with AM1.5 G filters set at 100 mW/cm^2 with a calibrated radiometer (IL 1400BL). Labview controlled *Keithley* 2400 SMU enabled the measurement of current density-voltage (J-V) curves every 4 s to observe any eventual curve modification during light exposure.

For the TiOx conductivity study, specific devices were fabricated using the following procedure. 15×15 mm^2 glass sheets are successively cleaned in acetone, ethanol, and isopropanol in an ultrasonic bath and exposed to UV-ozone for 20 min. Using the same titanium oxide precursor solution, a TiOx precursor layer is deposited by spin-coating (1000 rpm, 60 s) onto the glass sheets. After 2 h of conversion under air, the samples were put under an inert (N_2) atmosphere ([O_2] and [H_2O] < 0.1 ppm) and thermally treated at various temperatures from 80 °C to 180 °C for 10 min. Aluminum top contacts were then deposited by thermal evaporation in order to define the channel length and width, 50 μm and 2.5 mm, respectively. The I(V) characteristics of this devices, in the dark and under illumination, were recorded using a *Keithley 4200* SMU and the same solar simulator was used for solar cell characterization.

III. RESULTS AND DISCUSSION

A. Activation phenomenon

Figure 1(a) shows successive J-V curves of an inverted cell with untreated TiO_x measured under an inert

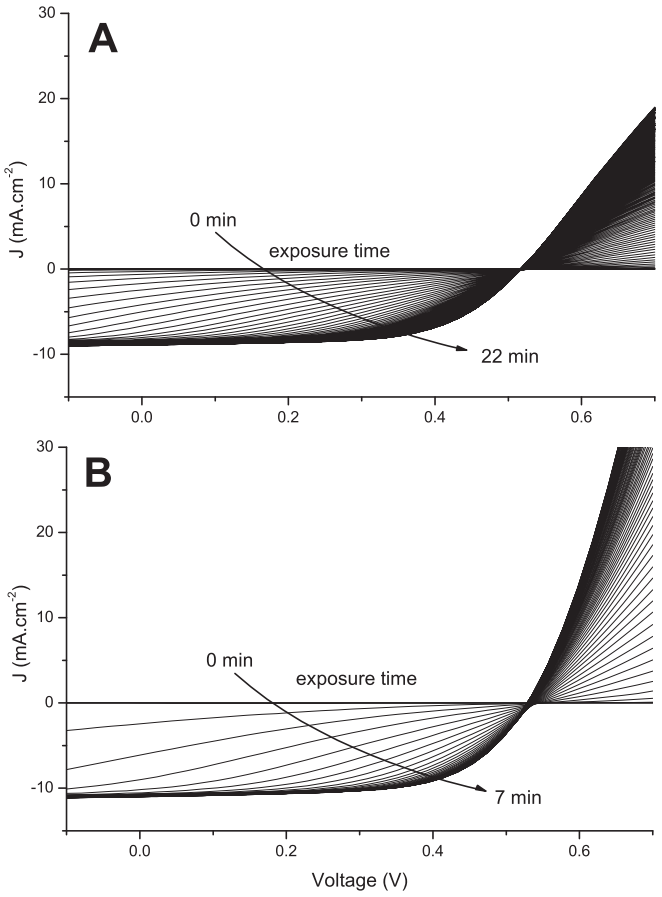

FIG. 1. Current density—voltage curves of solar cells upon light activation. Time delay between curves is 4 s. (a) Devices with pristine TiO_x and (b) devices with TiO_x pre-treated at 180 °C.

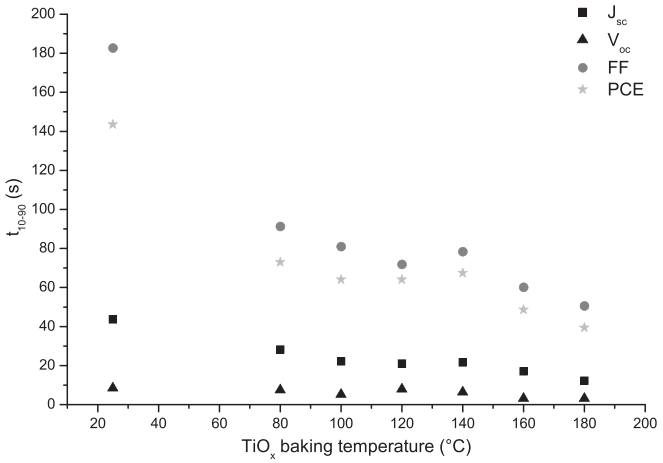

FIG. 2. Evolution of the rising time ($t_{10\text{-}90}$) for J_{sc}, V_{oc}, FF and PCE as a function of the baking temperature of TiO_x layer.

atmosphere. The first J-V curve does not show any significant rectification behavior under illumination nor in the dark. Thus, neither photocurrent nor photovoltage is initially measured. Overtime, short-circuit current (J_{sc}) slowly appears and increases up to reasonable values of 8.7 mA/cm^2 after 22 min of continuous light activation. These J-V curves suggest that the fill factor (FF) is strongly dependent on the light soaking while the open-circuit voltage (V_{oc}) and J_{sc} are less affected. The power conversion efficiency (PCE) of untreated TiO_x cells increases up to 2.8%. Figure 1(b) shows the same J-V curves recorded on cells with thermally treated TiO_x at 180 °C during 10 min under an inert atmosphere prior to the deposition of the bulk heterojunction. With the same time-lapse of 4 s between J-V curves, one observes a faster light activation. A similar increase of J_{sc} and FF is shown after 7 min of light activation to reach maximum output values V_{oc}, J_{sc}, FF and PCE of 0.53 V, 10.4 mA cm^{-2}, 0.63 and 3.5%, respectively.

In order to quantify the activation phenomenon, a rising time ($t_{10\text{-}90}$) for the different PV parameters (J_{sc}, V_{oc}, FF and PCE) was defined as the time needed for the value to increase from 10% to 90% of its maximum. Figure 2 presents the evolution of $t_{10\text{-}90}$ for J_{sc}, V_{oc}, FF, and PCE as a function of the baking temperature of the TiO_x layer. These results clearly show that V_{oc} reaches its maximum value after the first few seconds independently of the TiO_x baking time. This apparent Voc rising time is due to the fact that it is undetectable at the beginning as the device acts as an insulator. After a few seconds of illumination, the device starts to present a diode characteristic: the V_{oc} appears and does not change significantly upon further illumination. This is clearly different to the S-shape phenomenon observed in direct solar cells, in which the appearance of the S-shape anomaly is accompanied with changes in Voc. In those studies, the inflection points are attributed to the presence of interfacial dipoles.[16,17] Our result suggests that in TiO_x based devices the activation process is related to a vanishing of the insulating zone in series with the diode.

On the other hand, J_{sc} and FF (and as a consequence PCE) present a rising time dependent on the TiO_x baking temperature. Generally J_{sc} rises faster than FF and both rising times decrease with increasing TiO_x baking temperature. These rising times are considerably reduced if the TiO_x layer is pre-baked under an inert atmosphere at high temperatures (160–180 °C). Table I summarizes the average PV characteristics and their corresponding rising time for the different TiO_x baking temperature studied.

For all PV characteristics, an increasing TiO_x baking temperature leads to a shorter rising time. For unbaked devices, the $t_{10\text{-}90}$ of FF is much longer than that of the devices with TiO_x baked at 180 °C, 183 s, and 51 s, respectively. Liliedal *et al.* observed a similar effect of the thermal treatment on the activation of ZnO based OSC: thermal annealing at 105 °C leads to a less prominent inflection point in the IV. It was suggested that the desorption of molecular oxygen trapped at the surface of ZnO could occur thermally at 105 °C.[26] Our results are in agreement with this previous report and the decrease of the activation time with increasing temperature could be due to a faster desorption of molecular oxygen. This matter will be discussed in the next paragraph in which the deactivation experiments are analyzed.

Devices made with baked TiO_x layers also present better PV characteristics which is mainly due to an increase in the short-circuit current. Indeed, while devices with unbaked titanium oxide layers only reach 2.8%, almost all devices made with baked oxide layers present PCE above 3%. Moreover, it seems that starting from a baking temperature of 100 °C the devices PCE reach a plateau around 3.5% within error. AFM images of the different TiO_x layers were acquired and no relevant differences in the roughness of the surface were found, thus discounting the possible influence of the substrate morphology on the OSC performance.

TABLE I. J_{sc}, V_{oc}, FF and PCE (average values and standard deviation) and their respective $t_{10\text{-}90}$ for OSC devices with TiO_x unbaked and baked at 80, 100, 120, 140, 160 and 180 °C for 10 min.

T (°C)		RT	80	100	120	140	160	180
J_{sc}	mA · cm^{-2}	9.1 ± 0.6	10.2 ± 0.3	11.0 ± 1.3	11.8 ± 0.2	10.9 ± 0.7	9.7 ± 0.2	10.6 ± 0.3
	$t_{10\text{-}90}$ (s)	*44*	*28*	*22*	*21*	*22*	*17*	*12*
V_{oc}	mV	515 ± 5	513 ± 5	519 ± 4	520 ± 5	519 ± 6	515 ± 5	522 ± 5
	$t_{10\text{-}90}$ (s)	*8*	*7*	*5*	*8*	*6*	*3*	*3*
FF	Value	0.59 ± 0.02	0.61 ± 0.02	0.62 ± 0.01	0.58 ± 0.02	0.60 ± 0.02	0.59 ± 0.01	0.61 ± 0.01
	$t_{10\text{-}90}$ (s)	*183*	*91*	*81*	*72*	*78*	*60*	*51*
PCE	%	2.8 ± 0.3	3.2 ± 0.2	3.6 ± 0.5	3.6 ± 0.2	3.4 ± 0.3	2.9 ± 0.1	3.4 ± 0.1
	$t_{10\text{-}90}$ (s)	*144*	*73*	*64*	*64*	*67*	*49*	*39*

To conclude, a TiO_x-based OSC needs to be activated in order to give its optimal power conversion efficiency. This result indicates that traps are present in the titanium oxide layer or at the interface and that illumination of the TiO_x layer leads to the elimination or the filling of these traps. Interestingly, our study shows that increasing the annealing temperature of the TiO_x layer under an inert atmosphere leads to a lower activation time and improved PV characteristics. The next paragraphs focus on the origin of these traps and the influence of baking temperature on conductivity of the TiO_x layer.

B. Deactivation phenomenon

As the origin of the traps in TiOx is still under debate: adsorbed O_2,[21,27] shallow traps,[20] polarization,[19] the deactivation behavior of the activated OSC has been studied under different conditions. In this experiment, fully activated organic solar cells with unbaked TiO_x layers were kept under three different storage conditions in the dark: under an inert atmosphere at room temperature (N_2 – RT), under an inert atmosphere at 80 °C (N_2 – 80 °C) and under air at room temperature (Air – RT). Unbaked TiO_x based OSC were chosen for this study because of their extended activation time. The remaining activation rate (RAR) for each storage time is determined as the ratio between the PCE at $t = 0$ (first seconds of illumination) and the maximum PCE. Figure 3 shows the RAR as a function of the storage time under these different conditions. These results clearly show that the deactivation phenomenon is thermally dependent. Indeed, deactivation is the fastest when the device is stored at 80 °C under an inert atmosphere while an identical device, stored at room temperature and under the same inert atmosphere, does not deactivate, even after 100 h of storage. We emphasize that the same sample was submitted to successive activation/deactivation processes and that, for samples stored under inert atmosphere (N_2 – RT and N_2 – 80 °C), the whole study was carried out continuously under inert atmosphere, i.e., the samples were never in contact with the atmosphere. These

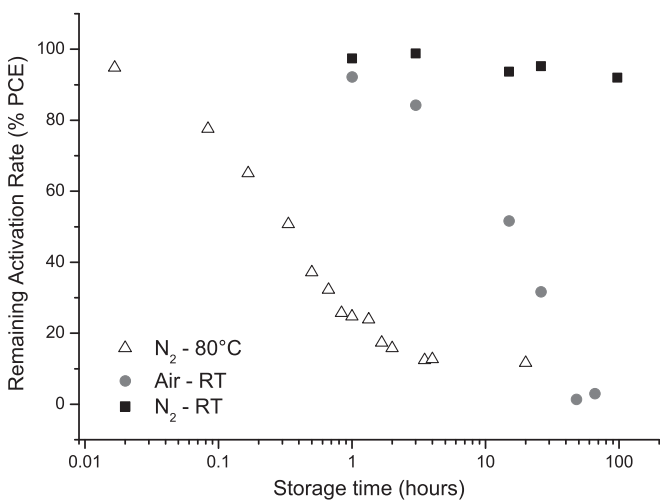

FIG. 3. Remaining Activation Rate as the function of the storage time under N_2 at room temperature (black squares), air at room temperature (grey circles) and N_2 at 80 °C (white triangles).

results prove that no irreversible physico-chemical modification of the materials or interfaces, such as sol-gel conversion completion or residual solvent removing for instance, is responsible for the activation phenomenon. It also rules out the intervention of O_2 as a trap, as suggested by Schmidt *et al.* and commonly accepted in ZnO based devices. Indeed, the activation/deactivation phenomenon at 80 °C and under an inert atmosphere is totally reversible. If O_2 is desorbed during the first activation cycle, it is unlikely that the oxygen molecules are re-adsorbed by treating the cell at 80 °C, especially under an inert atmosphere. Eisgruber *et al.* reported S-shape distortion in $CuInSe_2$ (CIS) solar cells which can only be removed by blue-light illumination, i.e., by photons with energy greater than the band-gap of CdS.[31] A model was proposed describing a high concentration of deep levels in the CdS window layer and a low concentration of free charge carriers. They also observed a long relaxation time due to a slow discharge rate of the deep states. Their observations and analysis are very similar to that observed in our study (white-light activation, slow deactivation at room temperature storage), suggesting that a similar process might occur in TiO_x based OSC. It is plausible that the amorphous TiO_x layer formed via sol-gel procedure contains deep electronic traps in the bandgap of TiOx. Irradiation in the UV range of the TiOx layer induces the direct excitation of valence band electrons into the conduction band. Both electrons and holes will then fill the traps. When the traps are totally filled, the free electron density in the conduction band is increased, the S-shape distortion disappears and the device presents its full performances. One may also note that storage under air at room temperature also provokes the deactivation of the device, even though it is at a different time scale. One might suggest that O_2 is adsorbed at the surface of the TiOx and would harvest an electron to formed O_2^-, therefore emptying traps.

Szczepankiewicz *et al.*[32] did an extensive study on the nature of the traps in TiO_2 layer. It was shown that, after irradiation of the TiO_2 layer and the creation of electron/hole pairs, both charges can be trapped by hydrated surfaces functionalities of TiO_2 according to the following mechanisms[32,33]:

$$h_{vb}^{+} + >Ti^{IV}OH \rightarrow \{>Ti^{IV}OH\cdot\}^{+}, \quad (1)$$

$$e_{cb}^{-} + >Ti^{IV}OH \rightarrow \{>Ti^{III}OH\}, \quad (2)$$

where $>Ti^{IV}OH$ represents the primary hydrated surface functionality of TiO_2, e_{cb} is the conduction band electron, h_{vb} is the valence band hole, $\{>Ti^{IV}OH\bullet\}^{+}$ is the surface trapped valence band hole and $\{>Ti^{III}OH\}$ is the surface trapped conduction band electron. These species are stable over time under different storage conditions. The trapped electrons in $\{>Ti^{III}OH\}$ species are only released upon illumination under O_2 and H_2O. Strong electron acceptor moieties such as Br_2 lead also to de-trapping while only O_2 does not. Although in the Szczepankiewicz *et al.* paper, TiO_2 was studied in a crystalline form, some similarities with our study can be observed. Actually, our results highlight the high stability of the trapped charges under inert atmosphere at room temperature. Even storage in air (in presence of O_2 and H_2O)

does not lead to a fast de-activation process, as shown by Szczepankiewicz *et al*. Based on the correlations between the two studies, one could suggest that the nature of the traps present in our devices are those resulting from reaction (1) and/or (2). In our study, TiO_x layer is amorphous. The trap density is thus higher than in a single crystal and $Ti^{IV}OH$ species might exist in the bulk and not only at the surface as it is the case for crystalline TiO_2. A basic storage in air is then less efficient to de-activate because either O_2 or H_2O have to diffuse in the bulk to release the charges in the traps. Further experiments will need to be performed in order to identify clearly the nature of the traps and quantify them.

C. Pure TiOx based devices

In order to investigate in detail the TiO_x activation phenomenon and the influence of baking the TiO_x under an inert atmosphere, TiO_x layers with aluminum contacts were fabricated with the architecture presented in the inset of Figure 4. Before the deposition of the aluminum contacts, the TiO_x layers were exposed to different baking temperatures under an inert atmosphere, from 80 °C to 180 °C in order to study its influence on the photoconduction of the TiO_x layers. The evolution of I(V) characteristics of unbaked and baked (80 °C to 180 °C) devices under illumination (100 mW cm^{-2}, AM 1.5 G, inert atmosphere) was investigated and the evolution of the conductance at a bias voltage of 1 V is plotted in Figure 4. It is clear that TiO_x devices have very low conductivity prior illumination. Conductance below 10^{-11} S is found in all cases before illumination, while it reaches up to 4×10^{-9} S after 9 min of illumination. Such a behavior had already been reported in a few articles on TiO_x-only devices.[34,35] Pomoni *et al*.[35] attributed the increase in the TiO_x photoconductivity upon illumination to traps filling until most of the traps are filled and the maximum photoconductivity is reached. In our experiments, the photoconductivity of baked and unbaked TiO_x layers increases similarly upon illumination; however, the activation rate and the maximum conductivity reached are influenced by the thermal treatment. For instance, baked TiO_x layers reach a higher photoconductivity than the unbaked device.

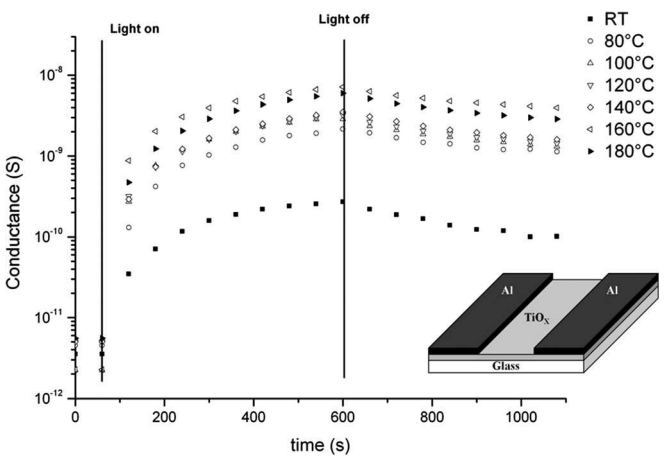

FIG. 4. Evolution of the conductance at a bias voltage of 1 V upon illumination for unbaked TiOx (■) and TiOx baked at 80 °C (○), 100 °C (Δ), 120 °C (▽), 140 °C ◁), 160 °C (▷) or 180 °C (•). Inset: Architecture of the TiO_x devices for the study of the activation phenomenon

The first observation is that light-activated baked TiO_x, even at low temperature such as 80 °C, present much higher conductivity than activated unbaked devices: there is at least one order of magnitude difference in the conductance. In addition, the higher the baking temperature, the better is the photoconductivity under illumination. Indeed, after the same illumination time, one can observe that the current increases gradually with the baking temperature, except for high temperature around 160–180 °C. Based on the hypothesis of Pomoni *et al*.,[35] one could suggest that the increase of the TiO_x baking temperature leads to the diminution of the trap density (primary hydrated surface functionality of TiO_2), and, therefore, to a faster attainment of high conductance values. Pomoni *et al*. also showed that the maximum photoconductivity reached is lower when the trap density is higher (in their case adsorbed O_2). This hypothesis is in agreement with the increase of the maximum conductivity with increasing baking temperature, i.e., decreasing trap density.

The second observation is that a persistent photoconductivity occurs. This phenomenon is a light-induced change in the free carrier concentration which persists once the light excitation is removed. This phenomenon has already been observed in GaN,[36,37] TiO_2,[38] and ZnO.[23] No systematic investigation has been made in this paper to explain the exact origin of the persistent photoconductivity. However, this behavior could be another signature of charges trapped in deep levels which are responsible of the light-activation phenomenon observed in inverted solar cells. A metastable state is activated with UV light in the TiO_x layer which acts as doping and reduces the series resistance of the inverted solar cell.

These changes in TiO_x conductivities can be linked to the differences observed in the OPV devices. Power conversion efficiencies vary from 2.8% for unbaked devices to more than 3% for devices with baked TiO_x. This increase can be explained by the better conductivity of baked TiO_x layers which would result in a lower series resistance, as observed in Figure 1. However, no obvious discrepancy is noticeable on the OSC photovoltaic characteristics versus the gradual increase of the TiO_x conductivity. Indeed, Table I indicates that devices with TiO_x baked at 100 °C present already very good PV characteristics. One can suggest that, above a specific conductivity of the TiO_x layer, other factors are limiting the PCE and the further increase of the TiO_x conductivity would have no influence on the PV characteristics, especially for thin TiO_x layers.[34]

From these results, it is also possible to understand the relation between the TiO_x baking temperature and the activation time. Data presented in Table I suggest that the conductivity of TiO_x layers baked at 100 °C is sufficient for the OSC to reach high performances and that the device presents 90% of its maximum PCE after 64 s of illumination. Figure 4 shows that after 1 min of illumination, the conductance of the TiO_x device under a 1 V bias is 2.7×10^{-10} S. The unbaked device reaches this value after more than 10 min of illumination while the device made with TiO_x baked at 80 °C reaches it between 2 and 3 min. For devices with TiO_x baked

at higher temperature, this value is reached in less than 1 min. As a conclusion, the higher the TiO_x baking temperature, the faster the TiO_x reaches the necessary conductivity and the faster the OSC device reaches its maximum performance.

IV. CONCLUSIONS

Thermal annealing under an inert atmosphere of TiO_x layer prior to active layer deposition is shown to shorten the activation period and to improve the overall performances of the devices. The baking process improves the conductivity of the TiO_x layer and explains the gain in performances and reduction of the activation time. Deactivation experiments were performed in order to understand the origin of the activation phenomenon. It was shown that activation/deactivation was fully reversible under an inert atmosphere and that deactivation was thermally assisted. The activation phenomenon is attributed to the presence of traps localized on the primary hydrated surface functionalities of TiO_x which have to be filled before the oxide reaches a sufficient conductivity, rather than desorption of O_2. Storage of the device under air leads to a slow deactivation of the OSC. One can suggest that adsorbed oxygen can empty the traps by creating O_2^- species. An optimal baking temperature of the TiO_x layer was found at 120 °C. In this case, OSC present a reasonable short activation time of approximately 1 min and an average PCE of 3.58% (a maximum PCE of 4%).

ACKNOWLEDGMENTS

This work has been supported by the French CNRS, the Région Aquitaine and the ANR through the ANR-10-HABISOL-003 «CEPHORCAS» project. The RHODIA Company (part of SOLVAY Group) is acknowledged for supporting part of the post-doctoral fellowship of Dr. Sylvain Chambon in our group. Finally, authors gratefully thank Sokha Khiev for his technical contribution to this work and Steven Meeker for his help to improve the language quality.

[1]G. Dennler, M. C. Scharber, and C. J. Brabec, Adv. Mater. **21**, 1323 (2009).
[2]Y. Sahin, S. Alem, R. de Bettignies, and J.-M. Nunzi, Thin Solid Films **476**, 340 (2005).
[3]G. Li, C. W. Chu, V. Shrotriya, J. Huang, and Y. Yang, Appl. Phys. Lett. **88**, 253503 (2006).
[4]M. S. White, D. C. Olson, S. E. Shaheen, N. Kopidakis, and D. S. Ginley, Appl. Phys. Lett. **89**, 143517 (2006).
[5]F. Zhang, X. Xu, W. Tang, J. Zhang, Z. Zhuo, J. Wang, J. Wang, Z. Xu, and Y. Wang, Sol. Energy Mater. Sol. Cells **95**, 1785 (2011).
[6]J. B. Kim, C. S. Kim, Y. S. Kim, and Y.-L. Loo, Appl. Phys. Lett. **95**, 183301 (2009).
[7]F. J. Zhang, D. W. Zhao, Z. L. Zhuo, H. Wang, Z. Xu, and Y. S. Wang, Sol. Energy Mater. Sol. Cells **94**, 2416 (2010).
[8]C. Y. Jiang, X. W. Sun, D. W. Zhao, A. K. K. Kyaw, and Y. N. Li, Sol. Energy Mater. Sol. Cells **94**, 1618 (2010).
[9]H. Oh, J. Krantz, I. Litzov, T. Stubhan, L. Pinna, and C. J. Brabec, Sol. Energy Mater. Sol. Cells **95**, 2194 (2011).
[10]R. Steim, S. A. Choulis, P. Schilinsky, and C. J. Brabec, Appl. Phys. Lett. **92**, 093303 (2008).
[11]P. de Bruyn, D. J. D. Moet, and P. W. M. Blom, Org. Electron. **11**, 1419 (2010).
[12]F. C. Krebs, Sol. Energy Mater. Sol. Cells **92**, 715 (2008).
[13]N. Sekine, C.-H. Chou, W. L. Kwan, and Y. Yang, Org. Electron. **10**, 1473 (2009).
[14]Z. Xu, L.-M. Chen, G. Yang, C.-H. Huang, J. Hou, Y. Wu, G. Li, C.-S. Hsu, and Y. Yang, Adv. Funct. Mater. **19**, 1227 (2009).
[15]H.-H. Liao, L.-M. Chen, Z. Xu, G. Li, and Y. Yang, Appl. Phys. Lett. **92**, 173303 (2008).
[16]A. Kumar, S. Sista, and Y. Yang, J. Appl. Phys. **105**, 094512 (2009).
[17]A. Wagenpfahl, D. Rauh, M. Binder, C. Deibel, and V. Dyakonov, Phys. Rev. B **82**, 115306 (2010).
[18]T. Kuwabara, T. Nakayama, K. Uozumi, T. Yamaguchi, and K. Takahashi, Sol. Energy Mater. Sol. Cells **92**, 1476 (2008).
[19]T. Kuwabara, C. Iwata, T. Yamaguchi, and K. Takahashi, ACS Appl. Mater. Interfaces **2**, 2254 (2010).
[20]C. S. Kim, S. S. Lee, E. D. Gomez, J. B. Kim, and Y.-L. Loo, Appl. Phys. Lett. **94**, 113302 (2009).
[21]H. Schmidt, K. Zilberberg, S. Schmale, H. Flugge, T. Riedl, and W. Kowalsky, Appl. Phys. Lett. **96**, 243305 (2010).
[22]Y. Jin, J. Wang, B. Sun, J. C. Blakesley, and N. C. Greenham, Nano Lett. **8**, 1649 (2008).
[23]F. Verbakel, S. C. J. Meskers, and R. A. J. Janssen, Appl. Phys. Lett. **89**, 102103 (2006).
[24]G. Lakhwani, R. F. H. Roijmans, A. J. Kronemeijer, J. Gilot, R. A. J. Janssen, and S. C. J. Meskers, J. Phys. Chem. C **114**, 14804 (2010).
[25]A. Manor, E. A. Katz, T. Tromholt, and F. C. Krebs, Sol. Energy Mater. Sol. Cells **98**, 491 (2012).
[26]M. R. Lilliedal, A. J. Medford, M. V. Madsen, K. Norrman, and F. C. Krebs, Sol. Energy Mater. Sol. Cells **94**, 2018 (2010).
[27]N. Golego, S. A. Studenikin, and M. Cocivera, Phys. Rev. B **61**, 8262 (2000).
[28]M. T. Dang, L. Hirsch, and G. Wantz, Adv. Mater. **23**, 3597 (2011).
[29]M. Burgos and M. Langlet, J. Sol-Gel Sci. Technol. **16**, 267 (1999).
[30]G. Li, Y. Yao, H. Yang, V. Shrotriya, G. Yang, and Y. Yang, Adv. Funct. Mater. **17**, 1636 (2007).
[31]I. L. Eisgruber, J. E. Granata, J. R. Sites, J. Hou, and J. Kessler, Sol. Energy Mater. Sol. Cells **53**, 367 (1998).
[32]S. H. Szczepankiewicz, A. J. Colussi, and M. R. Hoffmann, J. Phys. Chem. B **104**, 9842 (2000).
[33]M. R. Hoffmann, S. T. Martin, W. Choi, and D. W. Bahnemann, Chem. Rev. **95**, 69 (1995).
[34]M. Takahashi, K. Tsukigi, T. Uchino, and T. Yoko, Thin Solid Films **388**, 231 (2001).
[35]K. Pomoni, A. Vomvas, and C. Trapalis, Thin Solid Films **479**, 160 (2005).
[36]C. H. Qiu and J. I. Pankove, Appl. Phys. Lett. **70**, 1983 (1997).
[37]M. T. Hirsch, J. A. Wolk, W. Walukiewicz, and E. E. Haller, Appl. Phys. Lett. **71**, 1098 (1997).
[38]C. Itoh and A. Wada, Phys. Status Solidi C **2**, 629 (2005).